

1760 nm Multi-Watt Broadband PM CW and Pulsed Tm-doped Fibre Amplifier

Wiktor Walasik⁽¹⁾, Robert E. Tench⁽¹⁾, Gustavo Rivas⁽¹⁾, Jean-Marc Delavaux⁽¹⁾, Ian Farley⁽²⁾

⁽¹⁾ Cybel LLC, 1195 Pennsylvania Ave., Bethlehem, PA 18018 USA, wiktor.walasik@cybel-llc.com

⁽²⁾ Eblana Photonics Ltd., Laoghaire, Dublin, A96 A621, Ireland

Abstract We report the performance of CW and pulsed single-clad PM Tm-doped fibre amplifiers optimized for 1760–1960 nm wavelength band. We have achieved 3 W of CW output power and 20 W of peak power (1.6 μ J pulse energy, $\tau = 100$ ns, DC = 10%) at 1760 nm. Rectangular output pulses were achieved by using pulse preshaping technique. © 2022 The Author(s)

Introduction

Recent work in thulium-doped fibre amplifiers (TDFAs) demonstrates that these devices are capable of operation over a wide wavelength region spanning 1630 to >2100 nm [1–7]. While conventional TDFAs typically span 1850–2090 nm [5–7], extended wavelength TDFAs using custom research Ge/Tm co-doped silica fibres operate at wavelengths as low as 1630 nm [1–4]. TDFAs which readily access the 1730–1800 nm region are of particular interest because of rich molecular absorptions near 1730 and 1760 nm in CH₂ and other molecules that are quite significant for biophotonics applications [8–10]. Both CW and pulsed operation modes of the amplifier are important for biological physics and spectroscopy, for mid-IR frequency generation, for Raman soliton generation in conventional Si fibres, and for direct detection and coherent communications applications [9–14].

In this paper we propose and demonstrate a high-performance broadband PM TDFA operating at 1760 nm that uses standard commercially available Tm-doped fibres [5–7], has a fibre coupled output power as high as 3 W CW, has more than 20 W of peak power in the pulsed regime, and is constructed in an OEM package designed for immediate integration into existing laboratory setups. The pulse energies as high as 1.6 μ J were measured for 100 ns pulses emitted at the pulse repetition frequency (PRF) of 1 MHz. The pulse shape was corrected by preshaping the input pulses using an acousto-optic modulator (AOM) driven by an arbitrary wave generator (AWG).

Experimental Setup

Fig. 1 shows the configuration of the 1760 nm PM TDFA operated in a CW regime. This amplifier consists of a preamplifier stage followed by a booster stage. A 9-W 1567 nm fibre laser pump is split by a 75/25 passive coupler C1 to counter-pump (25%) the preamplifier stage and co-pump (75%) the booster stage via high power PM fused

fiber wavelength division multiplexers WDM1 and WDM2. Both amplifier stages use the same standard commercial 5 μ m core diameter PM TDF (ixblue IXF-TDF-PM-5-125). The gain fibres F1 and F2 are both 1 m long. In the current experiments, a PM circulator CIR was used as an interstage isolator. The third port of the isolator was used as a monitor for the backward emitted light from the booster stage. This will be replaced in the future by an interstage filter composed of a circulator CIR (note different orientation of the circulator outputs) and a narrow-band fiber Bragg grating (FBG) reflector. Both the input and output of the amplifier are protected from reflections by the PM isolators ISO1 and ISO2, respectively.

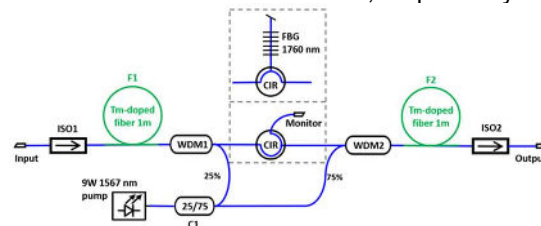


Fig. 1: Optical architecture of the two-stage PM 1760 nm TDFA.

CW performance of the dual-stage TDFA

Fig. 2 shows the experimental and simulation results obtained with the two stage PM TDFA. Up to 2.9 W of experimental fibre coupled output signal power was obtained with 4.75 mW of input power and 9 W of pump power, resulting in an external amplifier gain of 27.9 dB and optical-to-optical slope efficiency $\eta = 33.5\%$. While the simulated signal output power at maximum pump power is 8% (0.4 dB) higher than the experimentally measured power, the agreement between simulation and data is still good and is consistent with the previously observed agreement of 0.5 dB between theory and experiment [5–7]. The simulations show that the TDFA can deliver more than 3 W of output power in a broad range of wavelength between 1760 and 1960 nm.

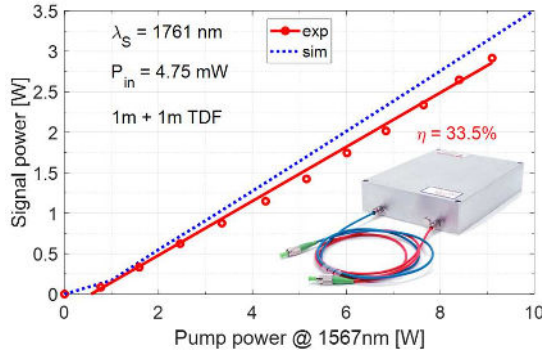


Fig. 2: Output signal power of the dual-stage TDFA vs 1567 nm pump power for 4.75 mW of CW input signal at 1761 nm. Inset shows the OEM package (200 x 150 x 43 mm³).

Fig. 3 shows the measured output spectrum of the amplifier. The measured OSNR at the signal wavelength is > 45 dB/1 nm. The ratio of the ASE power to the total output power decreases from 20% at low pump powers to less than 10% at 9W of pump power. The residual pump contributes below 2% to the total emitted power.

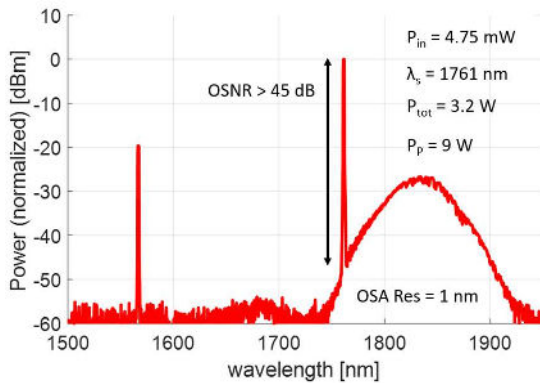


Fig. 3: Output spectrum of the dual-stage TDFA operating in CW mode.

Pulsed performance of the dual stage TDFA

Fig. 4 shows the schematic of the pulsed TDFA. In this experiment, we have operated the preamplifier in a CW mode to sufficiently saturate this first stage. We have inserted an AOM (Gooch and Housego) after the circulator, so that the input to the booster stage is pulsed. The AOM was optimized to operate at 2050 nm (where it has an insertion loss of 2.5 dB). In our experiments, it was operated at 1760 nm and displayed 6 dB of insertion losses. The AOM has rise/fall times around 10 ns. The third output of the circulator was used to monitor the backward emitted light from the power booster where stimulated Brillouin scattering (SBS) might occur. The electronic pulse shape driving the AOM was generated with an AWG.

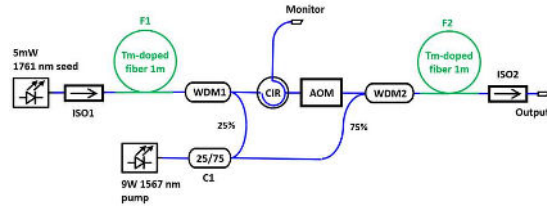


Fig. 4: Optical architecture of the TDFA operated in the pulsed regime.

Fig. 5 shows the output pulse energy measured at PRFs of 1 MHz (solid lines) and 2 MHz (dashed lines) with 10% duty cycle (DC). The red (blue) lines represent energy of the pulses obtained with a square (preshaped) input pulse. Up to 1.6 μJ of energy was measured at PRF of 1 MHz (pulse duration τ = 100 ns) and more than 0.9 μJ at PRF of 2 MHz (τ = 50 ns), which corresponds to more than 1.7 W of average output power. The pulse energy increases linearly with the pump power up to 1.5 μJ. Above that value the slope of the curve decreases slightly. The pulsed output spectrum at maximum power is similar to the CW spectrum shown in Fig. 3. The OSNR > 45dB/1nm was also observed, however the residual pump in the pulsed mode contributes up to 15% of the output power.

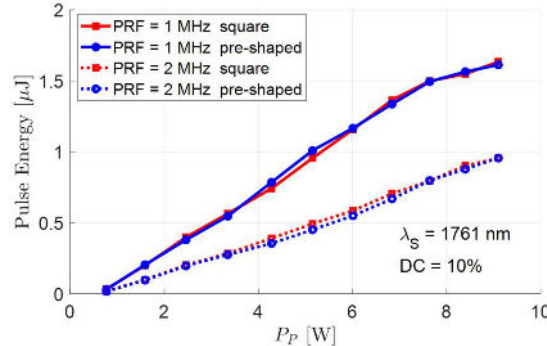


Fig. 5: Pulse energy emitted by the pulsed TDFA vs 1567 nm pump power for the input signal at 1761 nm operating at 1 and 2 MHz PRF.

Lowering the PRF while maintaining the pump power $P_p = 9$ W and DC = 10% allows for further increase of the peak power. At PRF of 100 kHz up to 190 W of peak power can be measured, however the pulse is strongly distorted by gain peaking and by the onset of SBS. To prevent these issues, we have used pulse preshaping, as demonstrated below.

Fig. 6 shows the output pulse shapes measured for the maximum pump power of 9 W at the pulse repetition frequencies PRF = 1 MHz. The pulses measured with a square input pulse (red) are compared with the AWG gain-equalized pulses (blue). We observe that input pulse pre-shaping using an AWG allows for efficient gain equalization of the output pulse. In case of the PRF = 1 MHz, the peak power is reduced from 31 to 19 W by the process of gain-equalization, which allows one to reduce the detrimental effects of the nonlinearities triggered by the high peak powers. Also, the pulse full width half maximum (FWHM) of the gain-equalized pulse is closer to the target pulse duration than in the case of the square input pulse. The 5% amplitude oscillation visible on top of the pulse has the oscillation frequency of 200 MHz, which corresponds to the drive frequency of the AOM.

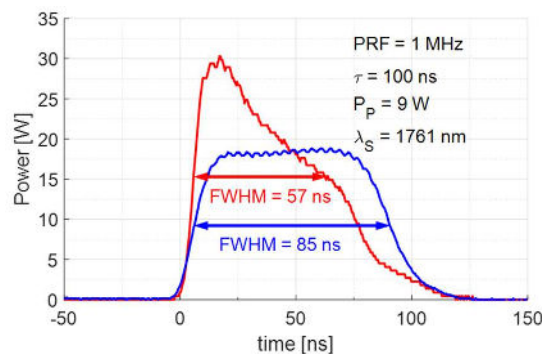


Fig. 6: Output pulse shapes from the pulsed TDFFA operated at 10% duty cycle measured at PRF of 1 MHz. The red (blue) curves show the output pulse shapes obtained with a square (pre-shaped) input pulse. Pulses were recorded with a Rigol MSO8104 oscilloscope.

Discussion

To our knowledge, this work represents the first report of ns AWG pulse-shaped polarization-maintaining TDFAs with multi-Watt level average output powers using a single-clad fibre with a small core diameter of 5 μm and in-band pumping at 1567 nm.

Previous ns pulsed work with single clad Tm-doped fibres employed non-PM 10 μm fibers pumped at 793 nm, exhibited 1 W average output power at 34 ns pulse width and 5 W average output power at 514 ns pulse width, both at 100 kHz repetition rate [15].

Other work on pulsed TDFAs and Tm-doped fibre lasers with ns pulse widths depends on the use of large core diameter (20-30 μm) double clad non-PM Tm-doped fibres in the output amplifier stage. For example, Li *et al.* demonstrated pulse widths of 100 ns and an average output power of 12.5 W at 25 kHz

repetition rate with a 25 μm double clad Tm-doped fibre amplifier pumped at 793 nm [16,17]. This experiment employed pulse shaping with an AWG and also direct source laser modulation and an electro-optic amplitude modulator to shape the input pulse. Wang *et al.* generated 156 ns pulses at a 1 MHz repetition rate with 105 W average output power, again using a 25 μm core diameter double clad Tm-doped fibre power amplifier pumped at 793 nm [18].

Our work is therefore the first example of multi-Watt level pulse-shaped single clad polarization-maintaining TDFAs in the 2 μm region of the spectrum using small core diameter 5 micron single clad TDFAs pumped in-band at 1567 nm. The use of practical, small core diameter, commercially available PM Tm-doped fibres pumped at 1567 nm with an uncooled fiber laser opens up many novel possibilities in both CW and pulsed TDFAs applications.

Summary and Conclusions

We have reported the performance of CW and pulsed single-clad PM Tm-doped fibre amplifiers optimized for the wavelength band from 1760 to 1960 nm. Output powers as high as 3 W CW and an OSNR > 55 dB/0.1 nm were achieved with our OEM packaged amplifier. In the pulsed mode, peak output powers as high as 20 W were measured in the 50-100 ns pulsed regime, corresponding to more than 1.6 μJ of pulse energy. The output pulse maintained a square pulse shape thanks to input pulse pre-shaping technique used. Our OEM TDFAs are pumped with an uncooled 1567 nm fibre laser which greatly enhances its areas of practical application. The future directions include increasing the generated peak power and pulse energies, and improving the pulse quality at low pulse repetition frequencies. This can be accomplished increasing the core size of the booster stage fibre to reduce the nonlinear effects.

With its high levels of CW and pulsed performance, our novel OEM packaged 1760 nm PM TDFAs can be immediately applied in experiments such as biological physics and spectroscopy, selective imaging of lipids and proteins by excitation of CH₂ in the 1730–1760 nm optical window, mid-IR frequency generation, Raman soliton generation in conventional Si fibres, and direct detection and coherent communications systems.

References

- [1] J. M. O. Daniel, N. Simakov, M. Tokurakawa, M. Ibsen, and W. A. Clarkson "Ultra-short wavelength operation of a thulium fibre laser in the 1660–1750 nm wavelength band", *Opt. Express*, vol. 23, no. 14, pp. 18269–18276, 2015, DOI: [10.1364/OE.23.018269](https://doi.org/10.1364/OE.23.018269)
- [2] Z. Li, A. M. Heidt, N. Simakov, Y. Jung, J. M. O. Daniel, S. U. Alam, and D. J. Richardson, "Diode-pumped wideband thulium-doped fiber amplifiers for optical communications in the 1800–2050 nm window", *Opt. Express*, vol 21, no. 22, pp. 26450–26455, 2013, DOI: [10.1364/OE.21.026450](https://doi.org/10.1364/OE.21.026450)
- [3] Z. Li, Y. Jung, J. M. O. Daniel, N. Simakov, M. Tokurakawa, P. C. Shardlow, D. Jain, J. K. Sahu, A. M. Heidt, W. A. Clarkson, S. U. Alam, and D. J. Richardson, "Exploiting the short wavelength gain of silica-based thulium-doped fiber amplifiers," *Opt. Lett.*, vol. 41, no. 10, pp. 2197–2200, 2016, DOI: [10.1364/OL.41.002197](https://doi.org/10.1364/OL.41.002197)
- [4] S. Chen, Y. Jung, S. Alam, D. J. Richardson, R. Sidharthan, D. Ho, S. Yoo, and J. M. O. Daniel, "Ultra-short wavelength operation of thulium-doped fiber amplifiers and lasers", *Opt. Express*, vol. 27, no. 25, pp. 36699–36707, 2019, DOI: [10.1364/OE.27.036699](https://doi.org/10.1364/OE.27.036699)
- [5] C. Romano, R. E. Tench, and J.-M. Delavaux, "Simulation of 2 μ m single clad thulium-doped silica fiber amplifiers by characterization of the 3F₄–3H₆ transition", *Opt. Express*, vol. 26, no. 20, pp. 26080–26092, 2018, DOI: [10.1364/OE.26.026080](https://doi.org/10.1364/OE.26.026080)
- [6] R. E. Tench, C. Romano, and J.-M. Delavaux, "Broadband 2-W Output Power Tandem Thulium-Doped Single Clad Fiber Amplifier at 2 μ m", *IEEE Photon. Technol. Lett.*, vol. 30, no. 5, pp. 503–506, 2018, DOI: [10.1109/LPT.2018.2801840](https://doi.org/10.1109/LPT.2018.2801840)
- [7] R. E. Tench, A. Amavigan, K. Chen, J.-M. Delavaux, T. Robin, B. Cadier, A. Laurent, "Experimental Performance of a Broadband Dual-Stage 1950 nm PM Single-Clad Tm-Doped Fiber Amplifier," *IEEE Photon. Technol. Lett.*, vol. 32, no. 15, pp. 956–959, 2020, DOI: [10.1109/LPT.2020.3006697](https://doi.org/10.1109/LPT.2020.3006697)
- [8] P. Wang, H.-W. Wang, M. Sturek, and J.-X. Cheng, "Bond-selective imaging of deep tissue through the optical window between 1600 and 1850 nm", *J. Biophotonics*, vol. 5, no. 1, pp. 25–32, 2012, DOI: [10.1002/jbio.201100102](https://doi.org/10.1002/jbio.201100102)
- [9] L. Wang, P. Lei, X. Wen, P. Zhang, and S. Yang, "Tapered fiber-based intravascular photoacoustic endoscopy for high-resolution and deep-penetration imaging of lipid-rich plaque," *Opt. Express*, vol. 27, no. 9, pp. 12832–12840, 2019, DOI: [10.1364/OE.27.012832](https://doi.org/10.1364/OE.27.012832)
- [10] J.T. Friedlein et al., "Dual-comb photoacoustic spectroscopy", *Nat. Commun.* vol. 11, pp. 3152, 2020, DOI: [10.1038/s41467-020-16917-y](https://doi.org/10.1038/s41467-020-16917-y)
- [11] L. Yang, Y. Li, B. Zhang, T. Wu, Y. Zhao, and J. Hou, "30-W supercontinuum generation based on ZBLAN fiber in an all-fiber configuration," *Photon. Res.* vol. 7, no. 9, pp. 1061–1065, 2019 DOI: [10.1364/PRJ.7.001061](https://doi.org/10.1364/PRJ.7.001061)
- [12] M. H. M. Shamim, I. Alamgir, and M. Rochette, "High Efficiency Raman Soliton Generation in Passive Silica Fiber," in 2021 Conference on Lasers and Electro-Optics Europe and European Quantum Electronics Conference, OSA Technical Digest (Optical Society of America, 2021), paper cd_2_3.
- [13] W. Walasik, D. Traoré, A. Amavigan, R. E. Tench, J.-M. Delavaux, and E. Pinsard, "2- μ m Narrow Linewidth All-Fiber DFB Fiber Bragg Grating Lasers for Ho- and Tm-Doped Fiber-Amplifier Applications," *IEEE J. Lightwave Tech.*, vol. 39, no. 15, pp. 5096–5102, 2021, DOI: [10.1109/JLT.2021.3079235](https://doi.org/10.1109/JLT.2021.3079235)
- [14] W. Walasik, R. E. Tench, G. Rivas, J.-M. Delavaux, and I. Farley, "1760 nm Multi-Watt Broadband PM Tm-doped Fiber Amplifier," to be published at CLEO 2022.
- [15] A. Sincore N. Bodnar, J. Bradford, A. Abdulfattah, L. Shah, and M. C. Richardson, "SBS Threshold Dependence on Pulse Duration in a 2053 nm Single-Mode Fiber Amplifier," *IEEE J. Lightwave Technol.*, vol. 35, no. 18, pp. 4000–4003, 2017, DOI: [10.1109/JLT.2017.2729508](https://doi.org/10.1109/JLT.2017.2729508)
- [16] Z. Li, A. M. Heidt, P. S. Teh, M. Berendt, J. K. Sahu, R. Phelan, B. Kelly, S. U. Alam, and D. J. Richardson, "High-energy diode-seeded nanosecond 2 μ m fiber MOPA systems incorporating active pulse shaping," *Opt. Lett.*, vol. 39, no. 6, pp. 1569–1572, 2016 DOI: [10.1364/OL.39.001569](https://doi.org/10.1364/OL.39.001569)
- [17] A. M. Heidt, Z. Li; D. J. Richardson., "High Power Diode-Seeded Fiber Amplifiers at 2 μ m—From Architectures to Applications," *IEEE JSTQE*, vol. 20, no. 5, pp. 525–536, 2014, DOI: [10.1109/JSTQE.2014.2312933](https://doi.org/10.1109/JSTQE.2014.2312933)
- [18] X. Wang, X. Jin, P. Zhou, X. Wang, H. Xiao, and Z. Liu, "105 W ultra-narrowband nanosecond pulsed laser at 2 μ m based on monolithic Tm-doped fiber MOPA," *Opt. Express*, vol. 23, no. 4, pp. 4233–4241, 2015, DOI: [10.1364/OE.23.004233](https://doi.org/10.1364/OE.23.004233)